Role of the Conserved Arginine 274 and Histidine 224 and 228 Residues in the NuoCD Subunit of Complex I from *Escherichia coli*

Galina Belevich, Liliya Euro, Mårten Wikström, and Marina Verkhovskaya*

Helsinki Bioenergetics Group, Institute of Biotechnology, University of Helsinki, P.O. Box 65 (Viikinkaari 1), Helsinki FIN-00014, Finland

Received October 4, 2006; Revised Manuscript Received November 15, 2006

ABSTRACT: The conserved arginine 274 and histidine 224 and 228 residues in subunit NuoCD of complex I from *Escherichia coli* were substituted for alanine. The wild-type and mutated NuoCD subunit was expressed on a plasmid in an *E. coli* strain bearing a *nuo*CD deletion. Complex I was fully expressed in the H224A and H228A mutants, whereas the R274A mutation yielded approximately 50% expression. Ubiquinone reductase activity of complex I was studied in membranes and with purified enzyme and was 50% and 30% of the wild-type activity in the H224A and H228A mutants, respectively. The activity of R274A was less than 5% of the wild type in membranes but 20% in purified complex I. Rolliniastatin inhibited quinone reductase activity in the mutants with similar affinity as in the wild type, indicating that the quinone-binding site was not significantly altered by the mutations. Ubiquinone-dependent superoxide production by complex I was similar to the wild type in the R274A mutant but slightly higher in the H224A and H228A mutants. The EPR spectra of purified complex I from the H224A and H228A mutants did not differ from the wild type. In contrast, the signals of the N2 cluster and another fast-relaxing [4Fe-4S] cluster, tentatively assigned as N6b, were drastically decreased in the NADH-reduced R274A mutant enzyme but reappeared on further reduction with dithionite. These findings show that the redox potential of the N2 and N6b centers is shifted to more negative values by the R274A mutation. Purified complex I was reconstituted into liposomes, and electric potential was generated across the membrane upon NADH addition in all three mutant enzymes, suggesting that none of the mutations directly affect the proton-pumping machinery.

NADH:ubiquinone oxidoreductase (complex I) is the entry point of reducing equivalents into the respiratory chain of mitochondria and many bacteria and catalyzes electron transfer from NADH to ubiquinone, which is coupled to translocation of 1.5−2 H^+ per e^- across the membrane (*1*−*3*). The molecular mechanism of proton translocation by this energy-converting enzyme is not known; two major kinds of hypotheses are currently under consideration. One employs tightly bound quinone(s), which is (are) located within the membrane dielectric (*4*, *5*). Reduction/oxidation of this quinone results in opening/closing of proton transfer pathways in the protein, which acquire protons from one side of the membrane and release them on the other; therefore, the bound quinone is the gate and the coupling site. In these views, the hydrophilic fragment of complex I only plays the role of an envelope for an electron-conducting "wire" consisting of eight to nine Fe-S clusters that starts from FMN and ends at iron−sulfur cluster N2 that is believed to directly interact with ubiquinone. An altogether different mechanism was proposed by Brand et al. (*6*, *7*), where energy conversion takes place in the hydrophilic fragment without involving tightly bound quinone. Ubiquinone from the membrane pool moves out along a "ramp" in the protein and reaches a quinone-binding site more than 40 Å away from the membrane, but in the vicinity of the N2 center. Electron transfer between N2 and the quinone results in conformational changes of the membrane fragment of complex I due to long-distance interactions, and proton translocation occurs upon relaxation of these conformational changes. According to this hypothesis, the protein surrounding of cluster N2 plays a critical role in energy transduction; therefore, this area of the protein is of particular interest. A number of conserved amino acid residues located in the vicinity of N2 and the proposed quinone-binding site were replaced by site-directed mutagenesis of the 49 kDa subunit of complex I from *Yarrowia lipolytica* (see ref *7* for a review). Two conserved histidines, H91 and H95, were found to be essential for ubiquinone reductase activity, whereas the properties of all Fe-S clusters determined by EPR spectroscopy remained unchanged by replacement of these histidines (*8*). It was suggested that these histidines may be partners for two conserved aspartates in the PSST subunit, participating in interaction between the 49 kDa and PSST subunits. However, no changes in the assembly or stability of mutated complex I were found (*8*). The highly conserved R141 was suggested to be located close to center N2, and this was confirmed when the 3D structure of the water-soluble fragment of complex I from *Thermus thermophilus* was resolved (*9*): the distance between center N2 and R141 (R84 in *T. thermophilus*) is only 5 Å (ref *9*; PDB code 2FUG). Replacement of R141 by alanine, methionine, and lysine was reported to

* To whom correspondence should be addressed: e-mail, Marina.Verkhovskaya@Helsinki.Fi; telefax, +358 9 191 58003; telephone, +358 9 191 59749.

10.1021/bi062062t CCC: $37.00
Published on Web 12/15/2006

Table 1: Bacterial Strains and Plasmids

strain or plasmid	genotype/relevant properties	ref
strains		
GR70N	F$^-$ *thi rps*L *gal*, wild-type complex I	*11*
GRC20	GR70N *nuoCD*::Zn^R	this study
GRC20R	CRC20/pBAD-nuoCD	this study
GRC-H224A	CRC20/pBAD-nuoCD(H224A)	this study
GRC-H228A	CRC20/pBAD-nuoCD(H228A)	this study
GRC-R274A	CRC20/pBAD-nuoCD(R274A)	this study
plasmids		
litmus 29	cloning vector, Ap^R	New England BioLabs
pBAD/HisA	expression vector, Ap^R	Invitrogen
pKO3	suicide plasmid, *sac*B, pSC101, Cm^R	*10*

cause loss of the N2 cluster, although quinone reductase activity of the mutated complex I remained significant (*8*). This is unexpected since center N2 is widely believed to be essential for ubiquinone reductase activity and to directly interact with ubiquinone. Brandt et al. suggested that this paradox could be resolved if another Fe-S cluster, foregoing N2 in the wire, resides at approximately 5 Å from N2; i.e., the gap in electron transfer would not be sufficient to limit turnover of complex I (about 100 s^{-1}) even if N2 is lost (*8*). However, this suggestion is not in agreement with the recent crystallographic data (*9*), which shows that the edge-to-edge distance between N2 and closest foregoing cluster N6b is 10.5 Å. The effects of the described mutations are hence contradictory, and further studies are clearly required. In this work we have substituted histidines H224 and H228, and arginine R274, for alanine in the NuoCD subunit of *Escherichia coli* complex I. The NuoCD subunit corresponds to a fusion of the 30 and 49 kDa subunits of the mitochondrial enzyme, and the mutants studied here correspond to the substitutions H91A, H95A, and R141A in the 49 kDa subunit of complex I from *Y. lipolytica*.

MATERIALS AND METHODS

Bacterial Strains and Site-Directed Mutagenesis. The bacterial strains and plasmids used in this study are listed in Table 1. All genetic manipulations, except for site-specific mutagenesis, were carried out using XL-1 Blue and TOP10 (Invitrogen) *E. coli* strains. The NuoCD-deficient strain GRC20 was constructed by deleting the internal part of the *nuo*CD gene from the chromosomal DNA of GR70N and replacing it by the unidirectionally transcribing zeocin resistance cassette using suicide plasmid pKO3, as described by Link et al. (*10*). The expression plasmid for in trans complementation of the deleted gene was prepared by amplification of the *nuo*CD gene from genomic DNA using primers CXhoF and CDBglR (Table 1) and subcloning of the PCR product, digested with *Xho*I and *Bgl*II, into litmus 29, generating LnuoCD. The *Xho*I−*Stu*I fragment from LnuoCD was ligated in *Xho*I−*Pvu*II sites of the expression vector pBAD/HisA (Invitrogen), resulting in pBAD-nuoCD. In-frame insertion of *nuo*CD was verified by DNA sequencing.

Point mutations were introduced into pBAD-nuoCD using the GeneEditor in vitro site-directed mutagenesis system (Promega) according to the manufacturer's instructions, followed by DNA sequencing of the mutated gene. The two histidines, H224 and H228, and arginine 274, were substituted for alanine. The oligonucleotides used for site-directed mutagenesis are listed in Table 2. In trans complementation was achieved by transformation of the NuoCD-deficient strain GRC20 by pBAD-nuoCD, bearing either the wild-type or mutated *nuo*CD gene resulting in the recovered GRC20R or mutant *E. coli* strains, respectively.

Table 2: Oligonucleotides Used in This Study

oligo-nucleotide	sequence[a]
CXhoF	5′-GCA**CTCGA**GAACAATATGACCGA
CDBglR	5′-GAT**AGATCT**GCGACCAACCGGCTGGC
H224A	5′-ACCTCGGTCCGAAC**GCG**CCGTCGGCGCACG
H228A	5′-GAACCACCCGTCGGCG**GCG**GGGGCTTTCC
R274A	5′-CCGTATACTGAC**GCG**ATCGAATACCTCG

[a] New restriction sites are underlined, and mutated nucleotides are in bold.

Bacterial Growth and Membrane Preparation. Bacteria were routinely grown in LB medium at 37 °C with appropriate antibiotics. The antibiotic concentrations (μg/mL) were as follows: ampicillin, 100; streptomycin, 50; zeocin, 50; chloramphenicol, 20. Growth tests were carried out under aerobic conditions at 37 °C in minimal medium containing DL-malate as the sole carbon source (*12*).

For membrane preparation and purification of complex I *E. coli* strain GRC20 transformed with pBAD bearing the wild-type or mutated *nuo*CD gene was grown aerobically in a 25 L fermentor in LB medium containing ampicillin at 37 °C. The cells were harvested in the second half of the exponential growth phase, washed with 0.5 M KCl and 10 mM Tris-HCl, pH 7.8, frozen as a pellet, and stored at −20 °C until use. Approximately 60 g of thawed cells was suspended in 250 mL of buffer containing 50 mM HEPES/KOH, pH 7.0, 100 mM KCl, 0.5 mM EDTA, and 0.5 mM PMSF[1] using UltraTurrax. Traces of DNase I were added to the suspension, and the cells were broken by passing through an APV Gaulin homogenizer at a pressure of 450 bar, 2 times 7 min. Unbroken cells and cell debris were removed by centrifugation at 11000*g* for 20 min, and membranes were sedimented from the supernatant by centrifugation at 200000*g* for 2.5 h. The obtained membrane pellet was suspended in 25 mM MES/BTP, pH 6.0, and 10 mM betaine, spun down again, and suspended in the same buffer at a protein concentration of 55−65 mg/mL. The membrane suspension was frozen in 1.5 mL aliquots in liquid N_2 and stored at −80 °C until use.

Purification of Complex I. The purification was based on procedures described in refs *12* and *13*. Thawed *E. coli* membranes were diluted to a protein concentration of 5 mg/mL in 50 mM MES/NaOH buffer with 0.5 mM PMSF, pH 6.0, and solubilized by the addition of DDM to 0.5% (w/v). After 10 min incubation at 4 °C under slow stirring, nonsolubilized material was removed by centrifugation for 30 min at 145000*g*. The supernatant was adjusted to 100 mM NaCl by dropwise addition of 5 M NaCl. The chroma-

[1] Abbreviations: HAR, hexaammineruthenium(III) chloride; DQ, decylubiquinone; DDM, *n*-dodecyl β-D-maltoside; PMSF, phenylmethanesulfonyl fluoride; dNADH, deaminonicotinamide adenine dinucleotide (reduced form); CCCP, carbonyl cyanide 3-chlorophenylhydrazone; WT, wild-type enzyme.

tography steps were carried out using the ÄKTAprime chromatography system (Amersham Biosciences). The membrane extract (approximately 170 mL) was loaded onto a 130 mL bed volume of a DEAE-Trisacryl M (BioSepra) anion-exchange column equilibrated with 50 mM MES/NaOH, pH 6.0, 100 mM NaCl, and 0.1% (w/v) DDM. The column was washed with 650 mL of 120 mM NaCl and eluted stepwise with 240 mL of 200 mM NaCl in the above buffer. Fractions with high NADH/HAR reductase activity (about 70 mL) eluting in a single peak were pooled, concentrated using Amicon Ultra-15 centrifugal filter devices (M_r cutoff 50 kDa), and adjusted to 100 mM NaCl by dilution with 50 mM MES/NaOH, pH 6.0, and 0.1% DDM. The adjusted sample was applied onto a 30 mL bed volume of a DEAE-Trisacryl M (BioSepra) column equilibrated with 50 mM MES/NaOH, pH 6.0, 100 mM NaCl, and 0.1% DDM. The column was washed with 150 mL of 130 mM NaCl and eluted using 70 mL of 180 mM NaCl in the above buffer. Fractions containing complex I (about 30 mL) were pooled and concentrated in Vivaspin-20 (M_r cutoff 100 kDa) to a protein concentration of 5 mg/mL. Then 0.5 mL aliquots were loaded onto 10.5 mL gradients of 15−30% sucrose in 50 mM MES/NaOH, pH 6.0, 100 mM NaCl, 5% glycerol, and 0.05% DDM and centrifuged for 20 h at 270000*g*. The NADH/HAR active fractions harvested from sucrose gradients were combined and concentrated without dilution using Vivaspin 20 (100 kDa cutoff) to a protein concentration of 4−8 mg/mL. Purified complex I was stored in small aliquots at −80 °C.

Measurements of Catalytic Activity. Complex I activity was measured at 30 °C in 1.4 mL of assay buffer containing 25 mM HEPES/BTP, pH 7.5 with constant stirring using a USB2000 UV−vis spectrophotometer (Ocean Optics, Inc). HAR and DQ reduction was measured by following NADH or dNADH oxidation (at 340 nm; $\epsilon = 6.2$ mM^{-1} cm^{-1}). HAR or DQ reduction in membranes and HAR reduction in purified mutated complex I were measured in an assay buffer containing 200 μM dNADH (NADH in the case of purified enzyme), 350 μM HAR, and 3.5 mM KCN or 50−60 μM DQ and initiated by the addition of 1−5 μg of protein. For the determination of DQ reductase activity and its inhibition by rolliniastatin purified complex I was activated by phospholipids: routinely 100 mg of solid asolectin was added to 1.8 mL of 200 mM HEPES/BTP, pH 7.0, containing 0.55% (w/v) sodium cholate and sonicated on ice until the solution was clear. Purified complex I was diluted by the cholate/phospholipid suspension to a concentration of 1−2 mg/mL, and the mixture was incubated for 20 min at room temperature. DQ reductase activity of purified activated complex I from mutants was studied in an assay buffer containing 11 μg/mL alamethicin, 50−60 μM DQ, 0.1 μg/mL bo_3 oxidase, and 1−3 μg/mL protein, and the reaction was initiated by the addition of 200 μM NADH. The concentration of rolliniastatin was determined as described in ref *14*. All experiments on activity characterization were reproduced three to four times.

Measurements of Superoxide Radical Generation. The formation of superoxide radical was monitored by the reduction of cytochrome *c* ($\epsilon_{550-539nm} = 21.5$ mM^{-1} cm^{-1}) in 1 mL of 25 mM HEPES/BTP buffer, pH 7.5, containing 100 mM KCl, 27 μM cyt *c*, 11 μg/mL alamethicin, 50−60 μM DQ (added where indicated), 0.1 μg/mL bo_3 oxidase, and 2−7 μg of activated purified complex I, and the reaction was started by the addition of 200 μM NADH. Measurements were done at 30 °C under constant stirring using a USB2000 UV−vis spectrophotometer (Ocean Optics, Inc). The rate of superoxide formation was determined as the superoxide dismutase-sensitive rate of cytochrome *c* reduction measured in pairs (with or without 20 units/mL superoxide dismutase).

Reconstitution of Complex I into Liposomes and Monitoring $\Delta\psi$ Generated by Complex I. Purified complex I at ∼8 mg/mL was mixed with the sonicated asolectin/cholate suspension in 200 mM HEPES/BTP, pH 7.0, in the ratio 1:4. The final concentration of asolectin and cholate was 44 mg/mL and 0.37%, respectively. After 15 min of equilibration, SM-2 Bio-Beads (Bio-Rad Laboratories) were added to a concentration of 300 mg of wet beads/mL, and the mixture was stirred gently for 2 h at room temperature. The orientation of reconstituted complex I was tested by measurements of NADH:HAR oxidoreductase activity in the presence and absence of alamethicin. It was found that 65−70% of complex I was incorporated into the liposomes with the hydrophilic fragment outward. The liposomes were used for monitoring $\Delta\psi$ by means of the electric potential-sensitive dye, Oxonol VI. Changes in absorption at 625−580 nm were measured with a Shimadzu dual-wavelength/double-beam UV3000 spectrophotometer. The assay contained 200 mM HEPES/NaOH, pH 7.0, 10 mM $(NH_4)_2SO_4$, 0.5 μM Oxonol VI, proteoliposomes (6 μg of complex I/mL), and 60 μM DQ.

Other Analytical Procedures. Protein concentrations were determined by the BCA protein assay reagent kit (Pierce) with bovine serum albumin as a standard.

EPR Spectroscopy. X-band EPR measurements (9.4 GHz) were performed with a Bruker EMS EPR spectrometer, equipped with an Oxford Instruments ESR900 helium flow cryostat with an ITC4 temperature controller. The field modulation frequency was 100 kHz and modulation amplitude 1.27 mT. The microwave power incident to the cavity is indicated on the figures. The spectra shown are normalized for temperature, gain, microwave power (*15*), and protein concentration and corrected for baseline. The spectral simulation was performed using Bruker Analytic GmbH software WinEPR SimFonia version 1.26 (beta). Samples of purified complex I (150 μL, 3−4 mg of protein mL^{-1}) were mixed with NADH (10 mM final concentration), transferred into EPR tubes, and frozen in liquid nitrogen. The complex I preparation was contaminated with the Fe-S protein of succinate dehydrogenase, the iron−sulfur clusters of which cannot be reduced with NADH without redox mediators. Therefore, in the EPR spectra of NADH-reduced complex I the signal of the oxidized 3Fe-4S cluster, S3, was subtracted from the final spectra.

RESULTS

Expression and Activity of Mutated Complex I. The wild-type or mutated NuoCD subunit was expressed on a plasmid in the *E. coli* strain bearing the *nuo*CD deletion. The expression of complex I can be estimated on the basis of the measurements of HAR reductase activity of the purified complex I and the membranes. Complex I with the H228A or H224A substitutions was fully expressed since the dNADH:HAR oxidoreductase activities in the membranes

Table 3: Activity of Wild-Type and Mutated Complex I in Membranes and Purified Enzyme

	activity, μmol of (d)NADH min^{-1} mg^{-1} (%)			
	WT	H224A	H228A	R274A
membranes				
dNADH:HAR reductase	1.90 ± 0.03 (100)	1.90 ± 0.05 (100)	1.83 ± 0.06 (96)	0.93 ± 0.05 (49)
dNADH:DQ reductase	0.85 ± 0.01 (100)	0.48 ± 0.05 (56)	0.28 ± 0.02 (33)	0.038 ± 0.001 (4.5)
purified complex I				
NADH:HAR reductase	96 ± 6 (100)	84 ± 1 (88)	98 ± 6 (100)	74 ± 3 (77)
NADH:DQ reductase[a]	25 ± 1 (100)	16 ± 2 (64)	12 ± 1 (48)	5.5 ± 1 (22)

[a] Complex I activated by phospholipids was used for the measurements.

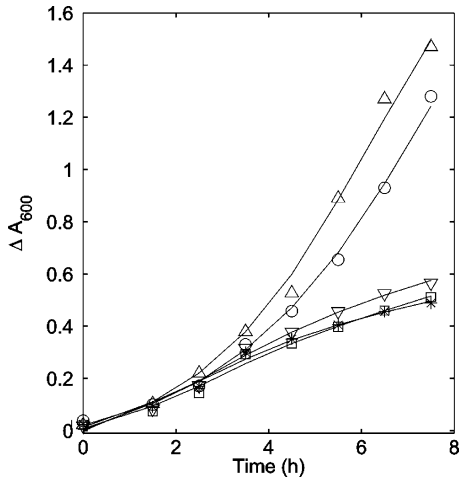

FIGURE 1: Growth of *E. coli* strains on malate with the mutated NuoCD subunit of complex I. Key: GRCR, wild type, circles; GRC-H224A, upward-pointing triangles; GRC-H228A, downward-pointing triangles; GRC20 (Δ*nuo*CD), squares; GRC-R274A, asterisks.

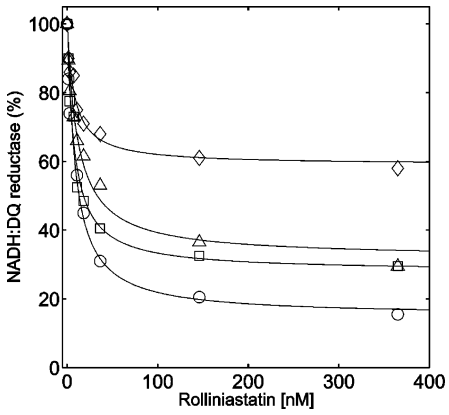

FIGURE 2: Inhibition of NADH:DQ oxidoreductase activity of purified wild-type and mutated complex I by rolliniastatin. Key: WT, circles; H224A, triangles; H228A, squares; R274A, diamonds.

and purified complex I from parent and mutated strains were equal (Table 3). The plasmid bearing *nuo*CD H224A was capable of recovering the complex I-deficient phenotype, i.e., growth on malate (Figure 1). Complex I with the R274A substitution was expressed by approximately 50%. Analysis on SDS−PAGE gels indicated that all subunits are present in complex I from all mutants (not shown). In membranes quinone reductase activity of mutated complex I was 56%, 33%, and 4.5% of wild type for H228A, H224A, and R274A, respectively. The purified complex I mutant enzymes showed NADH:HAR oxidoreductase activity close to that of wild type (77−100%) for all three substitutions, but the NADH:DQ activity was about half of wild type in H228A and H224A and about 20% in R274A (Table 3). These results differ from those reported for the corresponding mutants of complex I from *Y. lipolytica* (*8*) (see Discussion).

To test whether the quinone reductase activity in the mutants was due to nonspecific quinone reduction, the quinone-like inhibitor, rolliniastatin, was used. Titration of quinone reductase activity of purified complex I by rolliniastatin (Figure 2) showed that I_{50} was approximately the same in wild-type and mutated enzymes, in the range of 1.4−2.4 nM, which is close to the value found with bovine complex I (*14*). The same results were obtained with complex I in the native membranes (not shown). Although the proportion of the rolliniastatin-insensitive component of quinone reductase activity was higher in the mutated enzymes, especially in R274A, the absolute value of this component was not increased significantly; it was 3.8, 4.3, 3.4, and 3.3 μmol of NADH min^{-1} mg^{-1} for wild-type and H224A, H228A, and R274A mutant enzymes, respectively. This component probably reflects reduction of the artificial electron acceptor DQ that partially bypasses the normal route of reducing native ubiquinone.

Table 4: Superoxide Generation by Wild-Type and Mutated Purified Complex I

	$O_2^{\bullet-}$ generation, nmol of cyt *c* min^{-1} mg^{-1}	
strain	−DQ	+DQ
WT	22.9 ± 0.9	34.9 ± 0.1
H224A	18.5 ± 0.9	89.0 ± 1.0
H228A	24.8 ± 1	81.3 ± 3.9
R274A	26.1 ± 0.7	41.7 ± 3.0

If the rolliniastatin-insensitive component of the ubiquinone reductase activity (Figure 2) is due to unspecific reduction of ubiquinone in the water-soluble part of the protein, it should result in a drastic increase of superoxide production, as is the case upon Q_1 reduction by mitochondrial complex I (*16*). However, measurements of $O_2^{\bullet-}$ generation by mutated complex I from *E. coli* did not show significant changes (Table 4). Production of $O_2^{\bullet-}$ by wild-type and mutated enzymes in the presence of NADH and in the absence of added ubiquinone was practically the same. Addition of DQ resulted in a doubling of $O_2^{\bullet-}$ production in the H224A and H228A mutants, but $O_2^{\bullet-}$ production in R274A was very moderate. For comparison, addition of Q_1, known to undergo nonspecific one-electron reduction by complex I, resulted in a 6-fold increase of $O_2^{\bullet-}$ production by wild-type complex I (not shown). The insignificant difference in superoxide production by wild-type and R274A mutant enzyme is in good agreement with the data obtained on complex I from *Y. lipolytica* (*17*).

The results on complex I sensitivity to rolliniastatin and ubiquinone-dependent $O_2^{\bullet-}$ generation by the purified en-

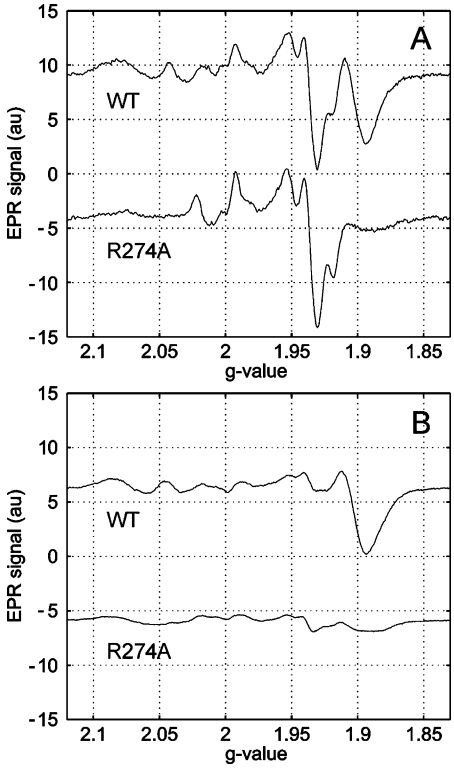

FIGURE 3: 10 K EPR spectra of NADH-reduced complex I from the wild-type and R274A mutant enzyme at low (A, 0.2 mW) and high (B, 10 mW) microwave power.

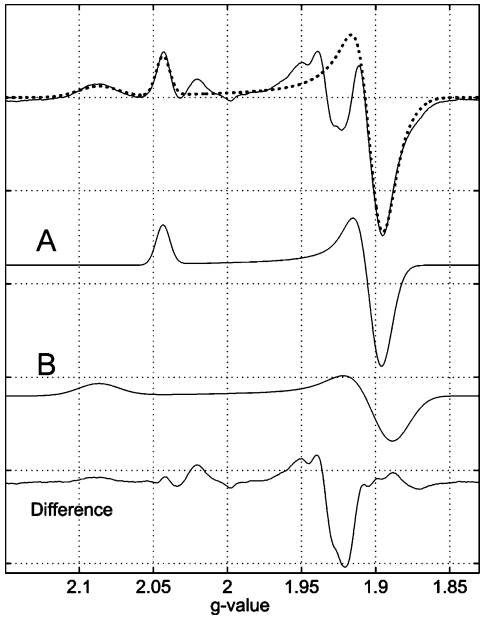

FIGURE 4: Simulation of fast-relaxing components of the NADH-reduced wild-type complex I spectrum with two individual signals. The complex I spectrum (solid line, upper trace) was obtained at 10 K and 10 mW. The individual spectra were simulated using the parameters $g_{xyz} = 1.900, 1.901, 2.045$ (A) and $g_{xyz} = 1.889, 1.905, 2.087$ (B). The dotted line represents the sum of the simulated spectra. The difference between the complex I spectrum and the sum (solid line, bottom trace) represents signals of slower relaxing Fe-S clusters.

zyme show that no significant change in accessibility of ubiquinone or modification of the quinone-binding site occurred upon the amino acid replacements.

EPR Properties of Mutated Complex I. NADH-reduced wild type and mutated complex I were used to study the EPR spectra of Fe-S clusters. The H224A, H228A, and R274A replacements did not affect the properties of [2Fe-2S] clusters since the spectra obtained at 45 K were identical in all preparations (not shown). Also, no significant difference was found between spectra of wild type and the H224A and H228A mutants at 10 and 5 K. The counterpart of R274 in complex I from *E. coli* is R141 in the 49 kDa subunit of complex I from *Y. lipolytica*, and its replacement with alanine was reported to drastically reduce the EPR signal of cluster N2 (*8*). We also observed that the bands at $g_z = 2.045$ and $g_{xy} = 1.89$ assigned to center N2 in the *E. coli* enzyme were almost completely lost in the R274A mutant enzyme. The spectra taken at low, 0.2 mW (Figure 3A), and high, 10 mW (Figure 3B), microwave power demonstrated that only fast-relaxing Fe-S clusters were disturbed; the other signals that belong to binuclear and slow-relaxing tetranuclear clusters were similar to signals from wild-type complex I. At 10 K two fast-relaxing [4Fe-4S] clusters contribute to the EPR spectrum of wild-type complex I reduced by NADH (Figure 4). Two signals with axial symmetry are seen, one of which corresponds to center N2 ($g_{xyz} = 1.900, 1.901, 2.045$) on the basis of its parameters reported in ref *18*. The assignment of the other cluster ($g_{xyz} = 1.889, 1.905, 2.087$) is uncertain (see Discussion). The sum of these signals fits well to the unsaturated component of the complex I spectrum. The difference between the experimental and simulated spectra derives from slower relaxing Fe-S clusters, since it has a different saturation behavior. The difference signal was microwave power dependent in the range 0.02−10 mW, whereas the amplitude of the bands of the fast-relaxing clusters was constant under these conditions. The spectrum of the NADH-reduced R274A mutant enzyme includes an unsaturated component derived from fast-relaxing Fe-S clusters (Figure 3, broad band around $g = 1.89$), but this signal is of very low amplitude and cannot be well fitted by combination of known individual spectra. Hence, both fast-relaxing clusters are disturbed by the R274A mutation. Brandt et al. (*8*), who also reported disappearance of the N2 signal in the corresponding mutant enzyme from *Y. lipolytica*, interpreted this finding as a loss of the N2 center, which appears reasonable due to its location close to the R274 residue (*9*). However, the loss of the EPR signal, which arises from the reduced cluster, might alternatively be caused by a substantial lowering of its midpoint redox potential (E_m). This explanation would be consistent with loss of positive charge in the vicinity of center N2, in which case it may no longer be reduced by NADH ($E_{m,7} = -320$ mV). To test this latter possibility, we reduced complex I with dithionite at pH 8.3, under which conditions the redox potential will be decreased to approximately −500 mV. Methylviologen (25 μM) was added as a redox mediator. Our preparation of complex I contained an Fe-S-containing protein as a contaminant, probably ferredoxin, that was rapidly reduced by dithionite, but not by NADH. On the other hand, complex I interacts with dithionite only slowly in the absence of methylviologen, and thus only the contaminant was reduced with dithionite. We therefore subtracted the spectrum of the dithionite-reduced preparation from the spectrum of the preparation reduced with dithionite and methylviologen to obtain a corrected spectrum of complex I at very low redox potential. Such spectra from wild type and the R274A mutant enzyme

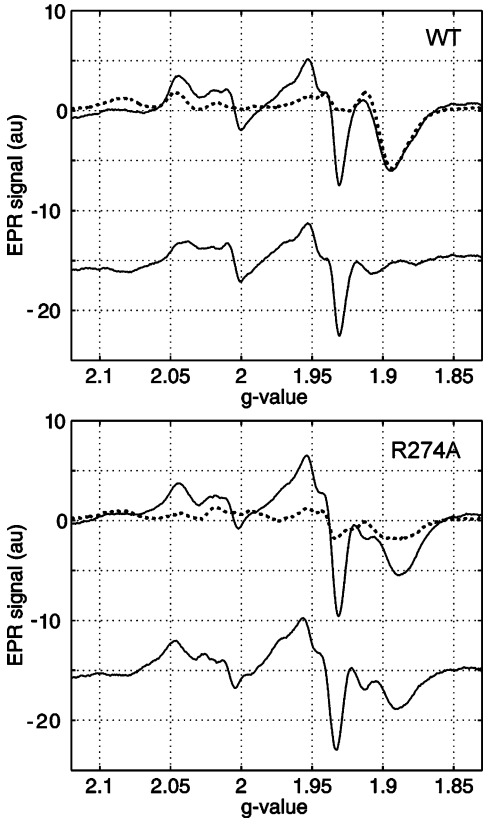

FIGURE 5: EPR spectra of complex I from wild type (upper panel) and from the R274A mutant (lower panel) reduced with dithionite in the presence of methylviologen (upper solid traces) and NADH (dotted traces). The spectra were obtained at 10 K and 10 mW. The difference between spectra of dithionite- and NADH-reduced complex I is shown by the lower solid traces.

are shown in Figure 5, from which the EPR signal of the methylviologen radical has been subtracted. For comparison, the spectra of both preparations reduced with NADH are shown by dotted lines. A new signal (trough at $g = 1.93$) not seen after NADH reduction appeared in both cases, belonging to a low-potential tetranuclear Fe-S cluster. The bands derived from center N2 and the other fast-relaxing cluster described above did not change significantly in the wild-type enzyme, which means that these clusters were already fully reduced with NADH. In contrast, the signals in the area of fast-relaxing clusters ($g = 2.045$ and $g \sim 1.89$) were strongly increased by dithionite plus methylviologen in the spectrum of the R274A mutant enzyme. Although this spectrum is reminiscent of that of center N2, it could not be simulated by known individual spectra from the wild-type enzyme, since the position of the trough was shifted to higher magnetic field and the band was broadened (see Discussion).

Reconstitution of Complex I into Proteoliposomes and Generation of Electric Potential by Complex I. Since the studied mutations reside at the suggested interface between the NuoB and NuoCD subunits, where the N2 center and the ubiquinone-binding site are located (*7*), and the electron transfer from N2 to ubiquinone was proposed to result in conformational changes coupled to proton translocation (*6*, *7*), these mutations might interfere with the latter function. To test this possibility, purified complex I was reconstituted into liposomes, and the generation of $\Delta\psi$ linked to NADH:DQ oxidoreduction was monitored by following changes in absorption of the electric potential-sensitive dye Oxonol VI.

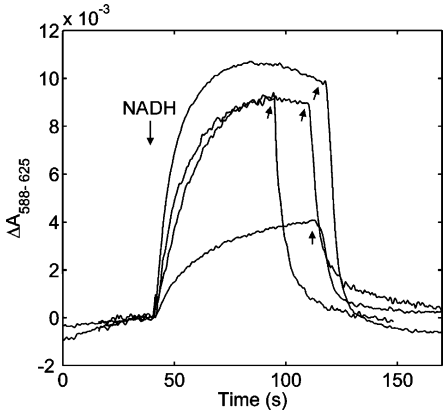

FIGURE 6: Generation of $\Delta\psi$ by wild-type and mutated complex I reconstituted into liposomes upon NADH oxidation by DQ. The reaction was initiated by the addition of 200 μM NADH as indicated by the downward arrow. Traces from top to bottom: WT, H228A, H224A, and R274A. The generated electric potential was dissipated by the addition of gramicidin (upward arrows show addition of 0.5 μg/mL gramicidin).

As shown in Figure 6, the addition of NADH in the presence of DQ resulted in $\Delta\psi$ generation that could be dissipated by gramicidin. All mutated enzymes generated $\Delta\psi$ although the amplitude of the response was different but correlated with the respective quinone reductase activity (Figure 6). Even complex I from the R274 mutant, whose activity was lower than 20% of wild type, generated $\Delta\psi$. Generation of $\Delta\psi$ by both wild-type and mutated enzymes was sensitive to both rolliniastatin and the uncoupler CCCP (not shown).

DISCUSSION

Comparison of the effects produced by mutations within the suggested ubiquinone-reducing catalytic core of complex I from *Y. lipolytica* and *E. coli* shows that some features of complex I vary and might therefore be organism-specific. We stress that analysis of corresponding mutations in different organisms is important because they may reveal common features of complex I that are relevant to the basic function of the enzyme. Replacement of the two conserved histidines, H228 and H224 in *E. coli* NuoCD, corresponding to H91 and H95 in the *Y. lipolytica* 49 kDa subunit, resulted only in a moderate decrease of ubiquinone reductase activity in *E. coli* in contrast to *Y. lipolytica*, where this activity was practically lost (*8*). Also, complex I from the H228A and H224A mutant enzymes retained its capability to translocate protons across the membrane, which does not support the notion of a central functional role of these residues. The recently resolved atomic 3D structure of the hydrophilic domain of complex I from *T. thermophilus* (*9*) allows determination of the location of H34 and H38 in the Nqo4 subunit, which are counterparts of H224 and H228 in the NuoCD from *E. coli*. These histidines are located at the edge of a "funnel" formed by Nqo4 (corresponding to NuoCD) and Nqo6 (corresponding to NuoB), the bottom of which abuts the membrane (Figure 7). This funnel is suggested to house the quinone-binding site (*9*). It seems reasonable that H224 and H228 might participate in quinone binding, as judged from the decrease in quinone reductase activity and the moderate increase in quinone-dependent superoxide production due to the replacement of histidine for alanine. However, neither histidine residue is likely to coordinate

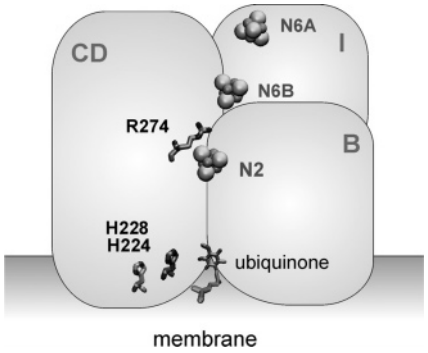

FIGURE 7: Relative location of three [4Fe-4S] clusters and mutated amino acid residues in subunits NuoI, NuoB, and NuoCD of complex I from *E. coli* and the membrane. The scheme is based on the 3D structure of the water-soluble domain of complex I from *T. thermophilus* (*9*).

ubiquinone directly since their replacement did not change the rolliniastatin sensitivity of the mutated enzymes in comparison to WT; these two histidines may rather participate in the interaction of the CD subunit with the membrane domain of complex I. On the other hand, replacement of R274 by alanine in NuoCD yielded more similar results to the corresponding mutation in *Y. lipolytica* (R141A, 49 kDa subunit). EPR spectra of complex I from the R274A mutant enzyme revealed a significant loss of the band assigned to the N2 cluster (Figure 3), as was the case for *Y. lipolytica*. The possibility that the replacement of the arginine with a neutral residue quite near N2 decreases the E_m of this cluster was tested by further reduction of the R141A mutant of *Y. lipolytica* with NADH plus dithionite, but no N2 signal appeared (*8*). In contrast, reduction by dithionite of the R274A mutant of the *E. coli* complex I resulted in a strong increase in the EPR signals of fast-relaxing [4Fe-4S] clusters, although these signals did not change in the wild-type enzyme by the same treatment. The signal at $g_z = 2.045$ that is part of the N2 signature grew as well as the g_y band at $g \sim 1.89$, although the position of the trough at $g = 1.89$ was shifted and the band was significantly broadened in comparison with the corresponding spectrum of the wild-type enzyme. These data show that cluster N2 is still present in the R274A mutant of complex I from *E. coli* but that its E_m is shifted to a much more negative value, as expected from the loss of positive charge, and that some of its properties are changed as seen by the slightly shifted EPR signature. This difference in relation to the mitochondrial complex I from *Y. lipolytica* is not known but might be due to poorer redox equilibration in the latter case, where the catalytic core is surrounded by several nuclear-encoded subunits, thus possibly preventing reduction of the low-potential N2 center. A similar phenomenon of negative shift in redox potential of N2 by replacement of a neighbor histidine to methionine was recently found by Zwicker et al. (*18*).

Analysis of the EPR spectra of fast-relaxing [4Fe-4S] clusters revealed that two clusters contributed to the bands at $g = 2.045$ and $g = 2.087$ and the wide band at $g \sim 1.9$ (Figure 4), which are strongly decreased by the R274A replacement (Figure 3). This means that another iron−sulfur cluster was disturbed in addition to N2. The characteristic EPR signal parameters of this second cluster are close to that reported for center N4 (*19*). However, the N4 cluster resides in the NuoG subunit (75 kDa, Nqo3) (*20*) and is located very far from R274. Moreover, no rigid elements such as an α-helix capable of transferring such a disturbance could be found in 3D structure of the water-soluble fragment of complex I (ref *9*; PDB code 2FUG). However, on the basis of the structure of the soluble domain of the *T. thermophilus* enzyme (*9*), center N6b located in NuoI (TYKY) is in the vicinity of N2 and R274 (Figure 7). Centers N6a and N6b were previously believed to be EPR silent as a result of strong electromagnetic coupling between them (*21*). However, as shown by Hinchliffe and Sazanov (*9*), the edge-to-edge distance between these centers is 9.4 Å, which should not result in very strong spin−spin interaction. Indeed, the analysis of site-directed mutations in the NuoI subunit of complex I from *Rhodobacter capsulatus* indicated two EPR-detectable [4Fe-4S] clusters bound to this subunit (*15*). Moreover, purified NQO9 (NuoI, TYKY) from *Paracoccus denitrificans*, after chemical reconstitution of Fe-S clusters, showed EPR spectra corresponding to two [4Fe-4S] clusters (*22*). Thus, the other cluster besides N2 that is perturbed by the R274A replacement could well be N6b, which is supported by its 8 Å distance from R274, not much different from the distance between R274 and center N2 (∼5 Å), as judged from the resolved structure (ref *9*; PDB code 2FUG).

ACKNOWLEDGMENT

We thank Dr. Moshe Finel and Kirsi Forsberg for help in construction of the NuoCD expression vector and the *nuo*CD deletion mutant and Anne Hakonen and Eija Haasanen for growing bacterial cultures and purification of complex I.

REFERENCES

1. Wikström, M. (1984) Two protons are pumped from the mitochondrial matrix per electron transferred between NADH and ubiquinone, *FEBS Lett. 169*, 300−304.
2. Galkin, A. S., Grivennikova, V. G., and Vinogradov, A. D. (1999) $H^+/2e^-$ stoichiometry in NADH-quinone reductase reactions catalyzed by bovine heart submitochondrial particles, *FEBS Lett. 451*, 157−161.
3. Bogachev, A. V., Murtazina, R. A., and Skulachev, V. P. (1996) H^+/e^- stoichiometry for NADH dehydrogenase I and dimethyl sulfoxide reductase in anaerobically grown *Escherichia coli* cells, *J. Bacteriol. 178*, 6233−6237.
4. Dutton, L. P., Moser, C. C., Sled, V. D., Daldal, F., and Ohnishi, T. (1998) A reductant-induced oxidation mechanism for Complex I, *Biochim. Biophys. Acta 1364*, 245−257.
5. Ohnishi, T., and Salerno, J. C. (2005) Conformation-driven and semiquinone-gated proton-pump mechanism in the NADH-ubiquinone oxidoreductase (complex I), *FEBS Lett. 579*, 4555−4561.
6. Brandt, U., Kerscher, S., Dröse, S., Zwicker, K., and Zickermann, V. (2003) Proton pumping by NADH:ubiquinone oxidoreductase. A redox driven conformational change mechanism?, *FEBS Lett. 545*, 9−17.
7. Brandt, U., Abdrakhmanova, A., Zickerman, V., Galkin, A., Dröse, S., Zwicker, K., and Kerscher, S. (2005) Structure-function relationships in mitochndrial complex I of the strictly aerobic yeast *Yarrowia lipolytica*, *Biochem. Soc. Trans. 33*, 840−844.
8. Grgic, L., Zwicker, K., Kashani-Poor, N., Kerscher, S., and Brandt, U. (2004) Functional significance of conserved histidines and arginines in the 49-kDa subunit of mitochondrial complex I, *J. Biol. Chem. 279*, 21193−21199.
9. Sazanov, L. A., and Hinchliffe, P. (2006) Structure of the hydrophilic domain of respiratory complex I from *Thermus thermophilus*, *Science 311*, 1430−1436.
10. Link, A. J., Phillips, D., and Church, G. M., (1997) Method for generation precise deletion and insertion in the genome of wild-type *Escherichia coli*: Application to open reading frame characterization, *J. Bacteriol. 179*, 6228−6237.

11. Green, G. N., Kranz, R. G., Lorence, R. M., and Gennis, R. B. (1984) Identification of subunit I as the cytochrome b_{558} component of the cytochrome *d* terminal oxidase complex of *Escherichia coli*, *J. Biol. Chem. 259*, 7994−7997.
12. David, P., Baumann, M., Wikström, M., and Finel, M. (2002) Interaction of purified NDH-1 from *Escherichia coli* with ubiquinone analogues, *Biochim. Biophys. Acta 1553*, 268−278.
13. Sinegina, L., Wikström, M., Verkhovsky, V. I., and Verkhovskaya, M. L. (2005) Activation of isolated NADH:ubiquinone reductase I (Complex I) from *Escherichia coli* by detergent and phospholipids. Recovery of ubiquinone reductase activity and changes in EPR signals of iron-sulfur clusters, *Biochemistry 44*, 8500−8506.
14. Esposti, M. D., Ghelli, A., Ratta, M., Cortes, D., and Estornell, E. (1994) Natural substances (acetogenins) from the family Annonaceae are powerful inhibitors of mitochondrial NADH dehydrogenase (Complex I), *Biochem. J. 301*, 161−167.
15. Chevallet, M., Dupuis, A., Issartel, J.-P., Lunardi, J., van Belzen, R., and Albracht, S. P. J. (2003) Two EPR-detectable [[4Fe-4S]] clusters, N2a and N2b, are bound to the NuoI (TYKY) subunit of NADH:ubiquinone oxidoreductase (Complex I) from *Rhodobacter capsulatus*, *Biochim. Biophys. Acta 1557*, 51−66.
16. Finel, M., Majander, A. S., Tyynelä, J., De Jong, A. M. P., Albracht, S. P. J., and Wikström, M. (1994) Isolation and characterization of subcomplexes of the mitochondrial NADH: ubiquinone oxidoreductase (complex I), *Eur. J. Biochem. 226*, 237−242.
17. Galkin, A., and Brandt, U. (2005) Superoxide radical formation by pure complex I (NADH:ubiquinone oxidoreductase) from *Yarrowia lipolytica*, *J. Biol. Chem. 280*, 30129−30135.
18. Zwicker, K., Galkin, A., Dröse, S., Grgic, L., Kerscher, S., and Brandt, U. (2006) The redox-Bohr group associated with iron-sulfur cluster N2 of Complex I, *J. Biol. Chem. 281*, 23013−23017.
19. Leif, H., Sled', V. D., Ohnishi, T., Weiss, H., and Friedrich, T. (1995) Isolation and characterization of the proton-translocating NADH:ubiquinone oxidoreductase from *Escherichia coli*, *J. Biochem*, *230*, 538−548.
20. Yano, T., Sklar, J., Nakamuro-Ogiso, E., Takahashi, Y., Yagi, T., and Ohnishi, T. (2003) Characterization of cluster N5 as a fast-relaxing [4Fe-4S] cluster in the Nqo3 subunit of the proton-translocating NADH-ubiquinone oxidoreductase from *Paracoccus denitrificans*, *J. Biol. Chem. 278*, 15514−15522.
21. Friedrich, T., Brors, B., Hellwig, P., Kintscher, L., Rasmussen, T., Scheide, D., Schulte, U., Mäntele, W. and Weiss, H. (2000) Characterization of two novel redox groups in the respiratory NADH:ubiquinone oxidoreductase (complex I), *Biochim. Biophys. Acta 1459*, 305−309.
22. Yano, T., Magnitsky, S., Sled', V. D., Ohnishi, T., and Yagi, T. (1999) Characterization of the putative 2 x [4Fe-4S]-binding NQO9 subunit of the proton-translocating NADH-quinone oxidoreductase (NDH-1) of *Paracoccus denitrificans*, *J. Biol. Chem. 274*, 28598−28605.

BI062062T